Impact of the Dissolved Anion on the Electrocatalytic Reduction of CO_2 to CO with Ruthenium CNC Pincer Complexes

Hunter Shirley,[a] Matthew T. Figgins,[c] Chance M. Boudreaux,[b] Nalaka P. Liyanage,[a] Robert W. Lamb,[c] Charles Edwin Webster,*,[c] Elizabeth T. Papish,*,[b] and Jared H. Delcamp*,[a]

[a] H. Shirley, Dr. N. P. Liyanage, Prof. J. H. Delcamp
Department of Chemistry and Biochemistry
Shelby Hall
The University of Alabama
University, MS 38677, USA
E-mail: etpapish@ua.edu

[b] C. M. Boudreaux, Prof. E. T. Papish
Department of Chemistry and Biochemistry
Shelby Hall
The University of Alabama
Tuscaloosa, AL 35487, USA
E-mail: delcamp@olemiss.edu

[c] M. T. Figgins, R. W. Lamb, Prof. C. E. Webster
Department of Chemistry
Hand Lab
Mississippi State University
Mississippi State, MS 39762, USA
E-mail: ewebster@chemistry.msstate.edu

Supporting information for this article is given via a link at the end of the document.

Abstract: The reactivity of three ruthenium electrocatalysts is shown to be modulated through the addition of anions for more selective and faster electrocatalysis. Controlled potential electrolysis studies confirm the generation of CO from CO_2. The Faradaic efficiency increased for the three ruthenium catalysts studied through the introduction of Cl^- to the reaction solution. Interestingly, a neutral ruthenium coordination complex with an associated chloride also gave equal or faster rates of catalysis upon Cl^- addition. In this report, a systematic study on the effects of added halides (I^-, Br^-, Cl^-, and F^-) with varied counter cations (K^+ and TBA^+) with and without water is examined. Computational analysis provides insights into this interesting increase in FE based on anion addition. These results show anion addition to electrocatalysis reaction mixtures add an additional parameter to increase both rate and selectivity of catalysis with one example improving from 19% FE to 91% FE for CO production.

1. Introduction

There is an urgent need to develop methods for the synthesis of renewable carbon-based fuels or fuel precursors (CH_4, CO, HCOOH, etc.) from the reduction of CO_2.[1] Electrocatalysis using heterogeneous or homogeneous catalysts provides a means for generating desirable fuels and fuel precursors. Homogeneous catalysts are attractive because a relatively rapid structure-function analysis is possible, which enables the rational design of catalysts for increased reactivity.[2] Changes to reaction conditions such as addition of cations and varying proton strength can have profound effects on catalyst kinetics, selectivities, and durabilities.[3] Additionally, anion selection could play a key role in modulating catalytic reactivity.

An increased understanding of catalyst behavior based on environmental changes to electrocatalytic reactions is needed to rationally design practical catalytic systems. Catalysts are often inherently exposed to water for systems that couple water oxidation to CO_2 reduction.[4] Thus, catalysts selective for the CO_2 reduction reaction (CRR) over the H^+ reduction reaction (HRR) are important.[2c, 3d, 5] This work seeks to compare the catalytic behavior of benchmark 2,2'-bipyridine (bpy)-ligated Ru-catalyst (**Ru-1**) and two bis(*N*-heterocyclic carbene) pyridinol-derived CNC-ligated Ru complexes (**Ru-2** and **Ru-3**) in the electrocatalytic CRR to understand the effect of added anions and water on the catalytic CRR (Figure 1).

The study of ruthenium-based molecular catalysts driving the CRR reaction remains an intense and attractive area of research.[6] Recent studies on the photocatalytic CRR with $[Ru^{II}(bpy)_2(CO)_2][PF_6]_2$ (**Ru-1**) and a pyridinol-derived pincer ligated ruthenium chloride complex (**Ru-2**) have revealed higher rates of reactivity and a higher durability of the pincer complex.[3b, 6j] Additionally, electrocatalysis appeared to be faster with **Ru-2** and halide-free **Ru-3** (vs. **Ru-1**) via preliminary cyclic voltammetry (CV) analysis.[6j] Access to the active catalyst via ligand dissociation is an important step for coordinateively saturated metal centers. This step is often presumed to be rapid halide dissociation for halide ligated complexes.[7] However, the same active catalyst as **Ru-3** may form if **Ru-2** undergoes rapid halide dissociation. Interestingly, a significant difference in the CRR with **Ru-2** and **Ru-3** is observed. This study seeks to probe halide effects further via electrocatalysis with two pincer complexes. A classic benchmarking catalyst is also studied to understand the generality of added anion effects.

Ru-1, **Ru-2**, and **Ru-3** have multiple monodentate, neutral, labile ligands which can dissociate. **Ru-2** has an additional halide ligand which may dissociate upon electrochemical reduction. Different active catalysts species could be formed from **Ru-2** and **Ru-3** depending on the group dissociated. Halides preferentially dissociate over neutral CO ligands with the widely studied

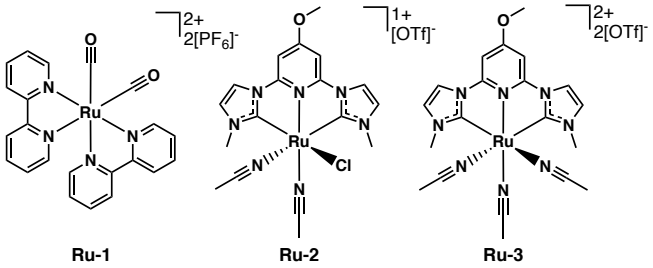

Figure 1. Structures of electrocatalysts **Ru-1**, **Ru-2**, and **Ru-3**.

$Re(bpy)(CO)_3Cl$.[7c, 8] Notably, cases are known where a significant difference in the reactivity of varied halide complexes exists.[9] Thus, addition of halides to the reaction medium could have a significant effect on the composition of the active catalyst depending on the binding strength of the halide. In this study, the two possible cases are probed computationally and experimentally: (1) **Ru-3** is a more active electrocatalyst than **Ru-2** due to lack of an anionic ligand dissociation step, and (2) different active catalysts are formed when staring with complexes **Ru-2** and **Ru-3** (Figure 2). Interesting findings based on similar hypotheses in other electrocatalysis manifolds have been reported in the literature.[10]

Results and Discussion

Cyclic voltammograms (CVs) under argon and CO_2 with **Ru-1**, **Ru-2**, and **Ru-3** were collected in the dark. A glassy carbon working electrode, silver wire, and platinum wire were used as the working, reference, and counter electrodes with a 0.1 M tetrabutylammonium hexafluorophosphate solution in acetonitrile. A scan rate of 100 mV/s is used in all the studies. Ferrocene was added as an internal reference at the end of each experiment. A 5% reaction solvent volume 2 M $KCl_{(aq)}$ solution was added when indicated. KCl was selected as the initial salt since the halide matches the **Ru-2** halide ligand. This avoids a potential mixed halide species from forming.

All three complexes show an electrochemically irreversible CV at the first reduction wave under argon or CO_2 (Figures S1-S2). Addition of $KCl_{(aq)}$ did not lead to reversible behavior and a current increase could be observed for **Ru-2** at the first reduction wave. The lack of reversiblity of the reduction waves suggests a chemical transfromation may take place following electron transfer to these complexes. Computational results indicate that this reduction event results in the loss of a mondentate ligand for each complex as either a Cl^- or MeCN ligand from **Ru-2 red.** and **Ru-3 red.** resulting in a significantly different potential to return to the Ru(II) oxidation state (Figures 2 and S20). Extending the CV window to more negative potentials reveals additional reduction waves for each complex (Figure 3).

The complexes have reduction onsets beginning at –2.0 to –2.4 V versus ferrocenium/ferrocene (Fc^+/Fc) under argon according to the following order: **Ru-1** < **Ru-3** < **Ru-2** (Figure 3). The onset of reduction is less negative by 0.2 V-0.7 V under CO_2 (Figure 3, Table 1). All catalysts show an increase in current when a CO_2 atmosphere (i_{cat}) replaces an argon atmosphere (i_p) with i_{cat}/i_p values ranging from 3.4-19.7 in the absence of $KCl_{(aq)}$ additive (Figure 3). Catalysts **Ru-1** and **Ru-2** have relatively modest increases in current under CO_2 at 3.9 and 3.4 times, respectively. **Ru-3** shows a dramatic increase in catalytic current

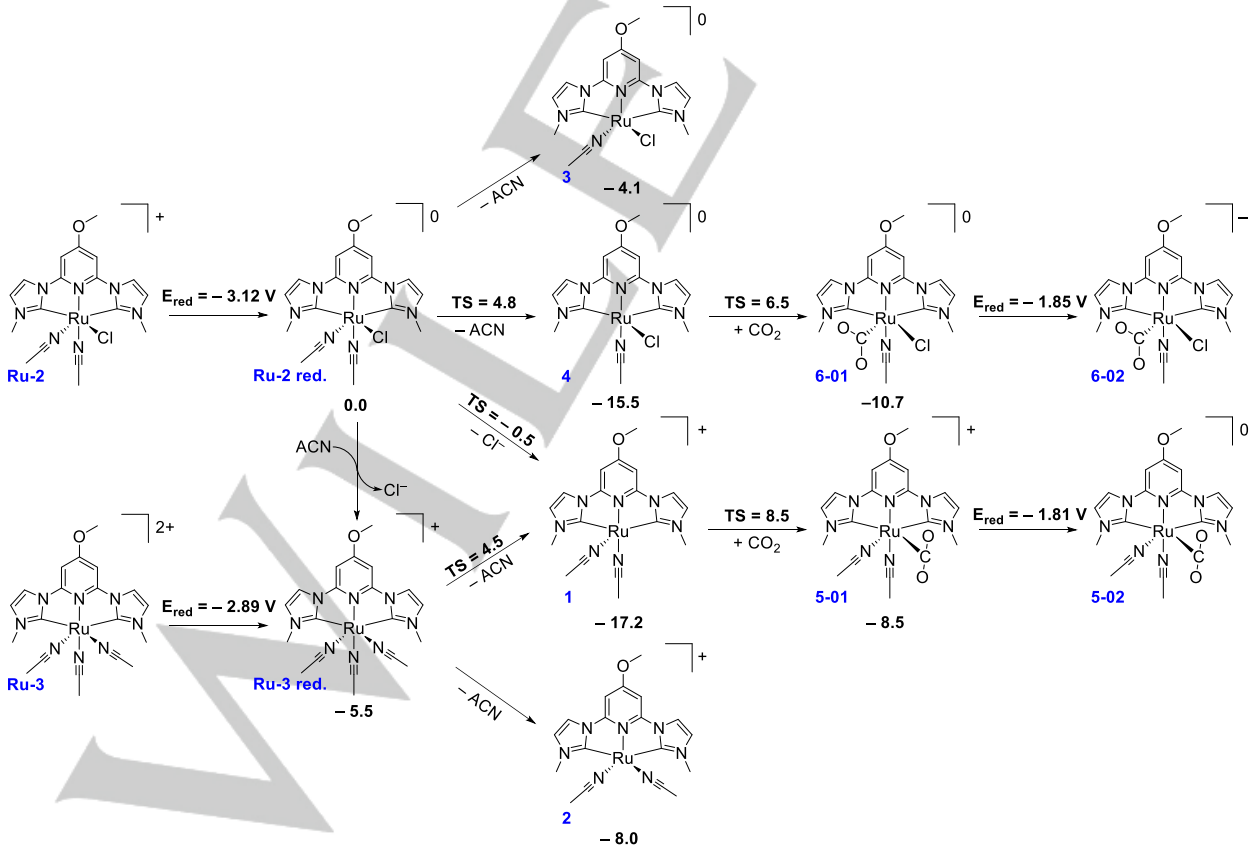

Figure 2. Initial steps for the electrocatalytic CRR beginning with **Ru-2** and **Ru-3**. Values are relative free energies in kcal/mol to **Ru-2 red.** with calculations at the SMD-PBE0-D3BJ/BS1 level of theory (see Experimental Section). Reported voltages are the half-cell reduction potentials of each species versus Fc^+/Fc.

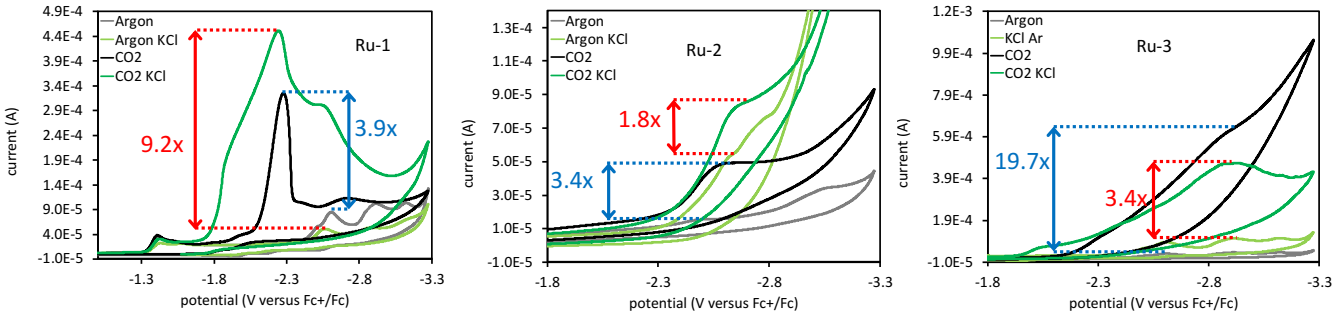

Figure 3. CV curves of **Ru-1**, **Ru-2**, and **Ru-3** in acetonitrile under Ar (gray without KCl; light green with KCl) and CO_2 (black without KCl and green with KCl).

Table 1. CV and CPE data with varied catalysts and additives.

entry	catalyst	additive	i_{cat}/i_p	$E_{RED\ CO2}$ onset (V)	$E_{RED\ CO2}$ peak (V)	CPE rate (C/h)	TON		FE (%)	
							CO	H_2	CO	H_2
1	**Ru-1**	none	3.9	-2.0	-2.3	4.9	0.8	0	19	0
2	**Ru-2**	none	3.4	-2.4	-2.6	1.1	0.4	0	11	0
3	**Ru-3**	none	19.7	-2.2	-2.9	1.7	0.7	0.3	17	5
4	**Ru-1**	+5% 2M $KCl_{(aq)}$	9.2	-1.7	-2.2	11.9	3.6	0.1	91	1
5	**Ru-2**	+5% 2M $KCl_{(aq)}$	1.8	-2.3	-2.7	21.1	1.5	2.6	38	65
6	**Ru-3**	+5% 2M $KCl_{(aq)}$	3.4	-1.9	-2.9	28.5	2.5	0	64	0

[a]All reactions were run until 3.8 C had passed with catalysts at a 1 mM concentration with a maximum TON value of 4 possible. **Ru-1** was electrolyzed at -2.2 V vs. Fc^+/Fc (ferrocenium/ferrocene) under anhydrous conditions and at -1.9 V with added 2 M $KCl_{(aq)}$. **Ru-2** and **Ru-3** were electrolyzed at –2.5 V and –2.7 V, respectively. All values are the average of at least 2 experiments.

by 19.7 times under CO_2. A current increase at the second reduction wave under CO_2 is observed for **Ru-1. Ru-2** and **Ru-3** have current increases at the first reduction wave, which is commonly observed for NHC ligated CRR catalysts.[3d, 11] Catalysis at the first reduction wave is possible if the initial complex reduction (first electron) is significantly more negative on the normal hydrogen electrode (NHE) scale than the CO_2 bound complex formed after the first reduction. This is substantiated by computational data showing the reduction of the CO_2 bound complexes being >1.0 V more positive for **Ru-2** and **Ru-3** (Figure 2). The i_{cat}/i_p ratio for **Ru-1** increased from 3.9 to 9.2 with a 300 mV shift to more positive potentials upon addition 2M $KCl_{(aq)}$. **Ru-2** and **Ru-3** show significant curve shape changes with added $KCl_{(aq)}$ resulting in more positive peak potentials and a slight lowering of i_{cat}/i_p values. Repeated CV cycling for 5 scans under CO_2 shows small changes in peak current amounts (Figure S3-S8). The changes are small which suggests the catalyst decomposition rate is slow on the CV time scale.

Controlled potential electrolysis (CPE) studies were used to verify the product composition (Figure 4, Table 1). A type 2 glassy carbon rod working electrode, an Ag reference electrode, and platinum foil counter electrode were used in these experiments (Figure S16). In each case electrolysis was run at a reduction potential corresponding to a catalyst wave peak in the CV with the CPE setup and until 3.8 C had passed. Only H_2 and CO were observed in these studies. **Ru-1** shows a modest amount of CO production under a CO_2 atmosphere at 0.8 turnover numbers (TONs) for CO with no additive, where TON = (moles of product)/(moles of catalyst) (Figure 4, Table 1). No H_2 was observed, and a Faradaic efficiency (FE) of 19% was found

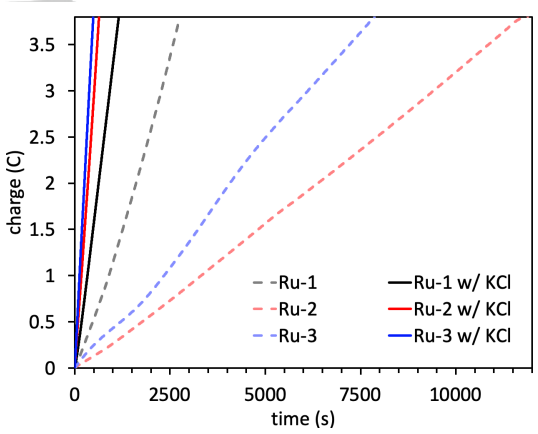

Figure 4. Charge versus time plots with and without 2 M $KCl_{(aq)}$ solution added.

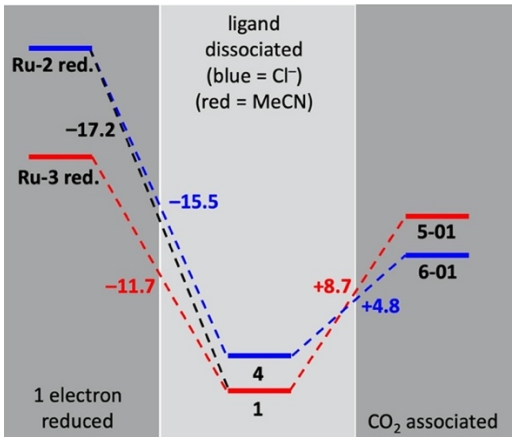

Figure 5. Thermodynamic diagram with the values listed in kcal/mol relative to the prior step.

where FE = [(moles of product)/(moles of electrons/2)]*100%. The location of the missing elecrons in this reaction is not apparent whereas HCO_2^-, CH_4, and MeOH were not observed. Additionally, catalyst deactivation via CO binding was probed after electrolysis via infrared spectroscopy studies (Figure S18).[6i, 12] No evidence of a Ru bound CO is apparent from these studies based on the lack of a signal at ~2000 cm^{-1}. Only trace MeCN is visible near this range at >2200 cm^{-1}. The TON value for CO increased to 3.6 with the observation of trace H_2 (0.1 TONs) upon addition of $KCl_{(aq)}$. The percent FE increased dramatically to 91% for CO with a rate change to 11.9 C/h from 4.9 C/h. The pincer ligated catalysts **Ru-2** and **Ru-3** passed charge slowly (1.1 C/h and 1.7 C/h, respectively) under anhydrous conditions with low TON and percent FE values (see Figure S17 for a current versus time plot). However, rate of charge passing during CPE increased substantially to 21.1 C/h for **Ru-2** and 28.5 C/h for **Ru-3** upon addition of 2 M $KCl_{(aq)}$. This increase in charge passage rate is accompanied by a significant increase in percent FE for the production of CO (**Ru-2** = 11% FE_{CO} without $KCl_{(aq)}$ and 38% FE_{CO} with $KCl_{(aq)}$; **Ru-3** = 17% FE_{CO} without $KCl_{(aq)}$ and 64% with $KCl_{(aq)}$). Notably, a sigifnicant portion of the charge balance could be accounted for as H_2 production at 65% FE in the presence of 2 M $KCl_{(aq)}$ with **Ru-2**. This indicates a low preference for CO_2 versus H^+ with **Ru-2**. Interestingly, **Ru-3** shows no H_2 production indicating a strong preference for the reduction of CO_2 over H^+ under identical conditions. These results suggest that **Ru-2** and **Ru-3** may opperate via two different mechanisms. One hypothesis for the difference in reactivity is a Cl^- ligand may be retained and a MeCN ligand dissociates from **Ru-2** to give a Cl-associated active catalyst. A second hypothesis is a different active site location could be opening on **Ru-2** and **Ru-3**. The active site could be trans to a MeCN ligand in the case of **Ru-2** upon reduction of the complex and loss of Cl^-. The active site could be trans to the pyridine ring in the case of **Ru-3**.

Computational data indicates that the dissociation of a Cl^- ligand from singly-reduced **Ru-2** is slightly favored over loss of a cis-to-pyridine MeCN ligand (by less than 2 kcal/mol; Figure 2). The transition state is approximately 5 kcal/mol higher in energy to access the chloride associated complex **4** relative to MeCN associated complex **1**. Similarly, dissociation of MeCN from singly-reduced **Ru-3** is thermodynamically preferential *trans* to an MeCN rather than *trans* to a pyridine group by more than 9 kcal/mol. Identical coordinatively-unsaturated active species (**1**) can be produced from either starting complex (Figure 2 and Figure 5). However, association of CO_2 is thermodynamically uphill from the coordinatively desaturated complexes **4** and **1** by 4.8 kcal/mol and 8.7 kcal/mol, respectively (Figure 5). This indicates CO_2 adduct formation is thermodynamically favored *trans* to a chloride rather than a MeCN group. It is possible that a significant number of complexes will still bear a Cl^- ligand during catalysis given that loss of MeCN or Cl^- from singly-reduced **Ru-2** are similar energetically.The transition state energies for binding CO_2 to **4** or **1** (6.5 and 8.5 kcal mol^{-1}, respectively) are only slightly above the energy required to remove the Cl^- or MeCN ligand (Figure 2 and Figure 5), but still positioned to be easily accessible, thus both **4** and **1** are expected to have appreciable populations at room temperature. Increasing the Cl^- concentration could favor a Cl-bound complex in solution resulting in changes in the CRR rates and product formation efficiencies if Cl^- is associating to an active catalyst species. Alternatively, a dissolved ion effect near the active catalyts site could alter reactivity.

Ru-3 was used for additional electrolysis studies to better understand if K^+, Cl^-, or H_2O is promoting faster catalysis. First, a series of potassium halide salts (KF, KCl, KBr, and KI) were added (Figures 6 and S9-S15, Table 2). The i_{cat}/i_p values follow the order: Cl^- > Br^- > I^- > F^- with a range of 3.4 to 1.3 being observed relative to the respective background reaction under argon for each KX salt. The observed halide trend does not follow the halogen periodic table group order. Interestingly, the free energy of dissociating each halide from a singly-reduced Ru complex correlates nicely with experimental data (Figure S19). These data suggest that the F^- counterion produces low catalytic activity because dissociation from the singly-reduced complex is quite endergonic (24.3 kcal/mol). Exergonic binding of additional F^- ligands to the complex could become irreversible, thus poisoning the catalyst. The I^-, Br^-, and Cl^- ions are each increasingly exergonic (ranging from –2.5 to –17.2 kcal/mol) to dissociate from the singly-reduced complex. It should be noted that the computed energies reported in Figure S19 will be affected by the ionic strength of the solution. Thus, the trend in these values could be fortuitous. Experimental results show clearly that when the K^+ and H_2O concentrations are held constant the value of i_{cat}/i_p can change by a factor of three based upon which halide is present. This demonstrates a clear dependence of the catalytic current increase on the halide present.

A series of CV scans under CO_2 were collected with added H_2O, tetrabutylammonium chloride (TBACl), and potassium hexafluorophosphate (KPF_6) to separate the effects of water, the cation, and the halide. First, H_2O was found to give no change in i_{cat} relative to i_p giving a non-catalytic i_{cat}/i_p value of 1.0. TBACl shows an i_{cat}/i_p value of 1.8 indicating the Cl^- likely has a significant effect on catalysis since the TBA ion is non-coordinating. Notably, $KPF_{6\,(aq)}$ leads to a higher i_{cat}/i_p value of 3.7 while $KPF_{6\,(MeCN)}$ gives a value of 1.0. These results indicate that: (1) the presence of Cl^- significantly effects current passing rates, and (2) the presence of both K^+ and H_2O leads to more current passage but neither component alone promotes current increases. To better understand this reactivity, CPE experiments were conducted to observed the products formed with these additives.

CPE experiments with H_2O, $KPF_{6\,(aq)}$, and $KPF_{6\,(MeCN)}$, pass significant amounts of charge but lead to low FE_{CO} values of ≤11% (Figure 7, Table 2). The product being formed as a result of the charge passing is not obvious in these cases with the maximum amount of H_2 being 27% FE_{H2}. However, addition of $TBACl_{(aq)}$ to the reaction gave a dramatically higher FE_{CO} at 70%. These results clearly show a uniquely strong influence of the Cl^- ion on catalytic reactivity and Faradaic efficiency. A possible origin of the Cl^- effect on the reaction may be due to formation of an active catalyst with a Cl^- associated from a complex with no halide associated before the CRR reaction began. Alternatively, a dissolved ion effect changing the environment near the active catalyst is possible. The approach of adding Cl^- to the CRR is a uniquely effective way to tune catalyst reactivity post synthesis with reaction conditions that could be generally applicable to CRR catalysis. In the case of **Ru-3**, a low FE catalyst (17%) could be significantly improved to 70% FE with respect to CO formation based on the addition of Cl^-.

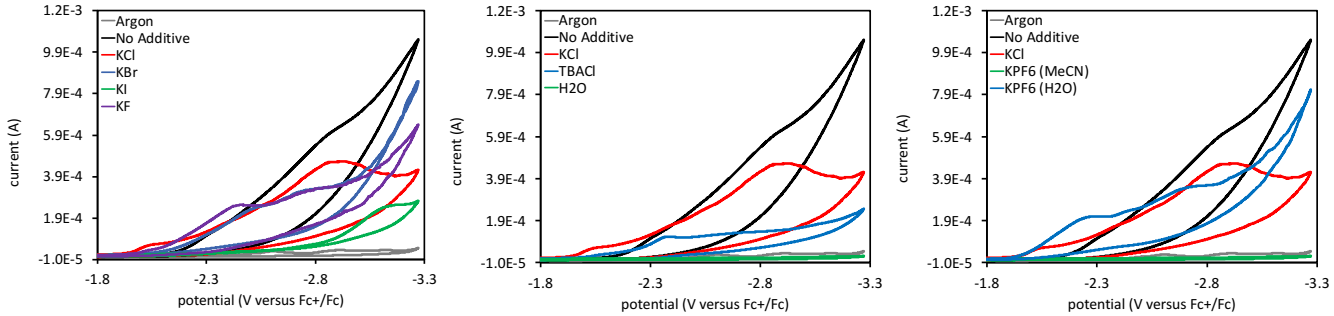

Figure 6. CV curves for catalyst **Ru-3**, measured in acetonitrile with 0.1 M *n*-Bu_4NPF_6 electrolyte under argon (gray) and CO_2 atmosphere (where the trace color corresponds to an additive).

Table 2. CV and CPE data for **Ru-3** catalyzed reactions with varying additives.

entry	additive	i_{cat}/i_p	E_{RED} onset (V)	E_{RED} peak (V)	CPE rate (C/h)	TON		FE (%)	
						CO	H_2	CO	H_2
1	none	19.7	-2.2	-2.9	1.7	0.7	0.3	17	5
2	+5% 2M KI (aq)	1.8	-2.0	-2.2	13.7	1.6	0	42	0
3	+5% 2M KBr (aq)	2.5	-1.7	-2.6	18.1	2.3	0	58	0
4	+5% 2M KCl (aq)	3.4	-1.9	-2.9	28.5	2.5	0	64	0
5	+5% 2M KF (aq)	1.3	-1.7	-2.1	6.2	1.5	0.3	38	8
6	+5% H_2O	1.0	-1.7	-1.8	5.3	0.2	1.1	5	27
7	+5% 2M TBACl (aq)	1.8	-1.7	-2.7	21.1	2.7	0	70	0
8	+5% 2M KPF_6 (aq)	3.7	-1.5	-1.7	114.0	0.5	0.6	11	16
9	+5% 2M KPF_6 (MeCN)	1.0	-1.6	-1.7	1.2	0.1	0.3	2	6

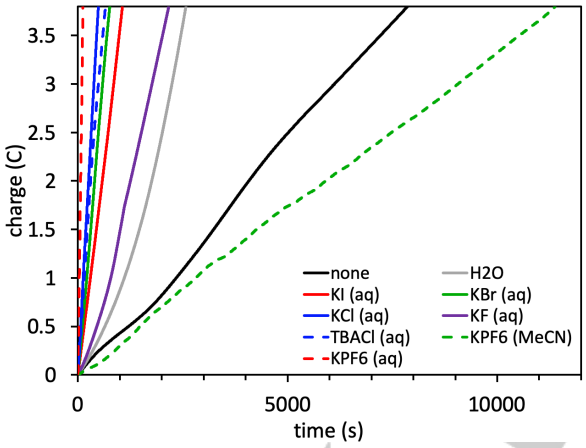

Figure 7. Charge versus time plot from CPE studies with varying additives with **Ru-3**.

Conclusion

Through electrochemical analysis the impact of various salt additives on the CRR with a ruthenium benchmark catalysts and two ruthenium pincer catalysts has been evaluated. Cationic, anionic, and H_2O effects were systematically tested. The composition of the halide anion was surprisingly found to play the dominate role in Faradaic efficiency values with improvements from as low as 19% without $KCl_{(aq)}$ additive to 91% with the additive. The chloride anion shows the greatest impact potentially due to encouraging active catalytic pathways where a halide bound intermediate is involved and a dissolved halide induced environmental change is favorable for CO production. Computational analysis reveals the formation of an active Cl^- bound catalyst is energetically plausible. Interestingly, either starting **Ru-2** or **Ru-3** complex could lead to similar active catalysts. However, the differences in reactivity in the electrocatalytic CRR suggest different active catalyst species may be present in solution. Additionally, the incorporation of a high concentration of dissolved Cl^- ions could be impacting the catalytic solvation environment favorably for increased reaction rates and increased selectivity for CO production.

Experimental Section

All computations were carried out using Revision B.01 of the Gaussian 16[13] suite of programs with default (10^{-8}) SCF convergence criteria. The PBE0 functional[14] was used in conjunction with Grimme's D3 empirical dispersion[15] and Becke-Johnson damping[16] [EMP=GD3BJ] for all computations. The basis set combination (BS1) is defined as follows: for Ru and Fe the Couty and Hall modification[17] (mod-LANL2DZ) to the valence basis set of LANL2DZ+ECP combination;[18] for Cl, Br, and I, when present, the LANL2DZ(d,p)+ECP combination;[19] and for C, H, N, O, and F, when present, the 6-31G(d')[20] basis sets (the 6-31G(d') basis sets have the d polarization functions taken from the 6-311G(d)[21] basis sets rather than the default value of 0.8[22] for C, N, O, and F). Spherical harmonic d functions were used throughout; *i.e.* there are 5 angular basis functions per d function. All geometries were fully optimized employing the SMD[23] implicit solvation model with parameters consistent with acetonitrile as the solvent. All stationary points were confirmed to be minima by an analytical frequency computation at the same level of theory. Reduction potentials for Ru complexes were determined by

calculating the absolute reduction potential of the Ru complex and subtracting the absolute reduction potential of the $Fc^{+/0}$ couple at the same level of theory using the relationship between free energy and electric potential.

$$\Delta G_{rxn} = -nFE$$

where ΔG_{rxn} is the free energy of the 1 electron reduction reaction

$$E^{\circ,comp}_{soln} = -\frac{\Delta G_{rxn}\ \text{kcal mol}^{-1}}{n\left(23.06 \frac{\text{kcal}}{\text{V mol}}\right)}$$

All commercially obtained reagents were used as received except MeCN which was freshly distilled before use over calcium hydride. Unless, otherwise noted, all electrolysis reactions were conducted under a CO_2 atmosphere and in the dark. Cyclic voltammetry was performed using a CH Instruments potentiostat (CHI-600E) with a glassy carbon electrode as the working electrode, platinum as the counter electrode, and Ag-wire as the pseudo-reference electrode with ferrocene as an internal reference. 0.1 M *n*-Bu_4NPF_6 is used as the supporting electrolyte and all the measurements were taken in acetonitrile. 3.0 ml of electrolyte solution at 1.0 mM catalyst concentration was used in each experiment. Before each measurement, the electrolyte solution was degassed with argon or CO_2 (~15 min). To avoid changes in concentration during degassing, pure acetonitrile (~5 mL) was first added to the electrolyte solution (3 mL) and the solution was degassed until the final total volume was reduced to 3.0 ml. CV measurements were taken at a scan rate 100 mV/s^{-1} and the sweep width window was set to ~100 mV past the second reduction potential for each catalyst. Utilization of distilled MeCN, analytically pure catalyst, and collection of CV data in the dark allows for reproducible CV traces as confirmed by multiple authors on this manuscript.

For CPE, all the measurements were performed with a CH Instruments electrochemical analyzer (CHI600E) and using a three-neck flask (50 mL) as the cell with rubber septum sealed electrode ports (Figure S16). The electrodes used are a platinum foil electrode as the counter electrode inside of a fine fritted isolation chamber, Ag wire as the reference electrode, and a glassy carbon 3 mm diameter carbon type 2 rod as the working electrode. Ferrocene (saturated in acetonitrile with 0.1 M tetrabutylammonium hexafluorophosphate in MeCN) was used as an electron source in the isolation chamber to avoid complete consumption of electrolyte during electrolysis. The height of solution in the isolation chamber (~2 mL) was even with the larger glassy carbon chamber solution level when the isolation chamber was fully submerged to avoid gravity assisted diffusion. To the glassy carbon chamber was added 6 mL of 0.1 M tetrabutylammonium hexafluorophosphate in acetonitrile solution. Pure acetonitrile (2 mL) was then added to the glassy carbon chamber along with 6 µmol of catalyst, and then the solution was degassed with argon or CO_2 (~ 15 min) until 2 mL of acetonitrile had evaporated from the glassy carbon chamber and a CV scan was taken at 100 mV/s to find the fixed potential to be used during CPE. During electrolysis, headspace samples (300 µL) were taken with a VICI valved syringe. The gas in the syringe was compressed to 250 µL, then with the tip of the syringe was submerged in a vial of diethyl ether, and the valve was opened to allow the pressure to equalize to atmospheric pressure. The entire 250 µL sample was then injected into a custom Agilent 7890B Gas Chromatograph (column, Agilent PorapakQ 6 ft, 1/8 OD) with a dual detector system (TCD and FID), a methanizer before the FID detector, and a backflush system. Quantitation of CO and CH_4 were made using an FID detector, while H_2 was quantified using a TCD detector. The CPE reactions were analyzed for formate as previously described and no appreciable amount was observed.[3b] In these studies, CO and H_2 were the only two appreciable products detected. All GC calibration standards were purchased from BuyCalGas.com. We note that in the CPE experiments could be reproduced with the use of an Ag reference electrode in an isolated aqueous KCl solution. However, the reproducibility using a reference electrode was lower than that of a bare wire presumably due to a trace water and KCl entering the electrolysis chamber. It should be noted that potential drift can be problematic during CPE using a pseudo-reference electrode in the electrolysis chamber. For this reason, the Coulombs passed was held constant in these studies, and a CV before and after electrolysis reveals modest drift amounts (0.05 V) for the amount of charge passed (Figure S17).

Acknowledgements

The authors thank the National Science Foundation for awards CAT-1800281, CAT-1800214, and CAT-1800201. The authors also thank the Mississippi Center for Supercomputing Research (MCSR) for access to computational resources. Preliminary results were obtained under NSF award OIA-1539035.

Keywords: electrocatalysis • carbon dioxide • reduction • pincer • anion effects

[1] a) M. Robert, *ACS Energy Lett.* **2016**, *1*, 281-282; b) A. M. Appel, J. E. Bercaw, A. B. Bocarsly, H. Dobbek, D. L. DuBois, M. Dupuis, J. G. Ferry, E. Fujita, R. Hille, P. J. Kenis, C. A. Kerfeld, R. H. Morris, C. H. Peden, A. R. Portis, S. W. Ragsdale, T. B. Rauchfuss, J. N. Reek, L. C. Seefeldt, R. K. Thauer, G. L. Waldrop, *Chem. Rev.* **2013**, *113*, 6621-6658.

[2] a) J. Qiao, Y. Liu, F. Hong, J. Zhang, *Chem. Soc. Rev.* **2014**, *43*, 631-675; b) N. Elgrishi, M. B. Chambers, X. Wang, M. Fontecave, *Chemical Society Reviews* **2017**, *46*, 761-796; c) H. Takeda, C. Cometto, O. Ishitani, M. Robert, *ACS Catal.* **2017**, *7*, 70-88; d) K. E. Dalle, J. Warnan, J. J. Leung, B. Reuillard, I. S. Karmel, E. Reisner, *Chem. Rev.* **2019**, *119*, 2752-2875; e) B. Zhang, L. Sun, *Chem Soc Rev* **2019**, *48*, 2216-2264; f) B. Das, A. Thapper, S. Ott, S. B. Colbran, *Sustainable Energy & Fuels* **2019**, *3*, 2159-2175; g) H. Ishida, C. Machan, M. Robert, N. Iwasawa, *Frontiers in Chemistry* **2020**, *8*, 59; h) E. E. Benson, C. P. Kubiak, A. J. Sathrum, J. M. Smieja, *Chem. Soc. Rev.* **2009**, *38*, 89-99; i) S. Zhang, Q. Fan, R. Xia, T. J. Meyer, *Acc Chem Res* **2020**, *53*, 255-264.

[3] a) M. Bourrez, F. Molton, S. Chardon-Noblat, A. Deronzier, *Angewandte Chemie International Edition in English* **2011**, *50*, 9903-9906; b) R. R. Rodrigues, C. M. Boudreaux, E. T. Papish, J. H. Delcamp, *ACS Appl. Energy Mater.* **2019**, *2*, 37-46; c) M. D. Sampson, C. P. Kubiak, *J. Am. Chem. Soc.* **2016**, *138*, 1386-1393; d) N. P. Liyanage, H. A. Dulaney, A. J. Huckaba, J. W. Jurss, J. H. Delcamp, *Inorg. Chem.* **2016**, *55*, 6085-6094; e) I. Bhugun, D. Lexa, J.-M. Saveant, *J. Am. Chem. Soc.* **1996**, *118*, 1769-1776; f) M. Hammouche, D. Lexa, M. Momenteau, J.-M. Saveant, *J. Am. Chem. Soc.* **1991**, *113*, 8455-8466; g) I. Bhugun, D. Lexa, J.-M. Saveant, *J. Phys. Chem.* **1996**, *100*, 19981-19985.

[4] a) X. Liu, S. Inagaki, J. Gong, *Angew. Chem. Int. Ed.* **2016**, *55*, 2-29; b) C. D. Windle, E. Reisner, *CHIMIA International Journal for Chemistry* **2015**, *69*, 435-441; c) V. Kumaravel, J. Bartlett, S. C. Pillai, *ACS Energy Lett.* **2020**, *5*, 486-519.

[5] a) N. Elgrishi, M. B. Chambers, M. Fontecave, *Chem Sci* **2015**, *6*, 2522-2531; b) T. Shimoda, T. Morishima, K. Kodama, T. Hirose, D. E. Polyansky, G. F. Manbeck, J. T. Muckerman, E. Fujita, *Inorg. Chem.* **2018**, *57*, 5486-5498; c) C. Costentin, S. Drouet, M. Robert, J. M. Saveant, *Science* **2012**, *338*, 90-94; d) S. I. Johnson, R. J. Nielsen, W. A. Goddard, *ACS Catal.* **2016**, 6362-6371; e) S. T. Ahn, E. A. Bielinski, E. M. Lane, Y. Chen, W. H. Bernskoetter, N. Hazari, G. T. Palmore, *Chem. Commun.* **2015**, *51*, 5947-5950; f) V. S. Thoi, C. J. Chang, *Chem. Commun.* **2011**, *47*, 6578-6580.

[6] a) Y. Kuramochi, O. Ishitani, H. Ishida, *Coord. Chem. Rev.* **2018**, *373*, 333-356; b) G. Sahara, O. Ishitani, *Inorg. Chem.* **2015**, *54*, 5096-5104; c) Y. Kuramochi, J. Itabashi, K. Fukaya, A. Enomoto, M. Yoshida, H. Ishida, *Chem Sci* **2015**, *6*, 3063-3074; d) S. K. Lee, M. Kondo, G. Nakamura, M. Okamura, S. Masaoka, *Chem. Commun.* **2018**; e) S. K. Lee, M. Kondo, M. Okamura, T. Enomoto, G. Nakamura, S. Masaoka, *J. Am. Chem. Soc.* **2018**; f) M. R. Madsen, J. B. Jakobsen, M. H. Rønne, H. Liang, H. C. D. Hammershøj, P. Nørby, S. U. Pedersen, T. Skrydstrup, K. Daasbjerg, *Organometallics* **2020**; g) Z. Chen, C. Chen, D. R. Weinberg, P. Kang, J. J. Concepcion, D. P. Harrison, M. S. Brookhart, T. J. Meyer, *Chem. Commun.* **2011**, *47*, 12607-12609; h) S. Gonell, M. D. Massey, I. P. Moseley, C. K. Schauer, J. T. Muckerman, A. J. M. Miller, *J. Am. Chem. Soc.* **2019**, *141*, 6658-6671; i) S. Gonell, E. A. Assaf, K. D. Duffee, C. K. Schauer, A. J. M. Miller, *J. Am. Chem. Soc.* **2020**, *142*, 8980-8999; j) C. M. Boudreaux, N. P. Liyanage, H. Shirley, S. Siek, D. L. Gerlach, F. Qu, J. H. Delcamp, E. T. Papish, *Chem. Commun.* **2017**, *53*, 11217-11220; k) S. Lense, K. I. Hardcastle, C. E. MacBeth, *Dalton Trans* **2009**, 7396-7401; l) Y. Tamaki, D. Imori, T. Morimoto, K. Koike, O. Ishitani, *Dalton. Trans.* **2016**, *45*, 14668-14677; m) G. J. Barbante, P. S. Francis, C. F. Hogan, P. R. Kheradmand, D. J. Wilson, P. J. Barnard, *Inorg. Chem.* **2013**, *52*, 7448-7459; n) R. Kuriki, H. Matsunaga, T. Nakashima, K. Wada, A. Yamakata, O. Ishitani, K. Maeda, *J. Am. Chem. Soc.* **2016**, *138*, 5159-5170; o) M. Riklin, D. Tran, X. Bu, L. E. Laverman, P. C. Ford, *Journal of the Chemical Society, Dalton Transactions* **2001**, 1813-1819.

[7] a) S. Sato, T. Morikawa, T. Kajino, O. Ishitani, *Angew. Chem. Int. Ed.* **2013**, *52*, 988-992; b) S. Sato, T. Morikawa, *ChemPhotoChem* **2017**; c) Y. Kou, Y. Nabetani, D. Masui, T. Shimada, S. Takagi, H. Tachibana, H. Inoue, *J. Am. Chem. Soc.* **2014**, *136*, 6021-6030.

[8] H. Takeda, K. Koike, H. Inoue, O. Ishitani, *J. Am. Chem. Soc.* **2008**, *130*, 2023-2031.

[9] a) A. J. Huckaba, E. A. Sharpe, J. H. Delcamp, *Inorg. Chem.* **2016**, *55*, 682-690; b) H. Shirley, T. M. Sexton, N. P. Liyanage, C. Z. Palmer, L. E. McNamara, N. I. Hammer, G. S. Tschumper, J. H. Delcamp, *Eur. J. Inorg. Chem.* **2020**, DOI: 10.1002/ejic.202000283; c) J. G. Vaughan, B. L. Reid, P. J. Wright, S. Ramchandani, B. W. Skelton, P. Raiteri, S. Muzzioli, D. H. Brown, S. Stagni, M. Massi, *Inorg. Chem.* **2014**, *53*, 3629-3641.

[10] a) B. Das, A. Orthaber, S. Ott, A. Thapper, *ChemSusChem* **2016**, *9*, 1178-1186; b) B. Das, A. Orthaber, S. Ott, A. Thapper, *Chem. Commun.* **2015**, *51*, 13074-13077; c) T. A. White, S. Maji, S. Ott, *Dalton Trans* **2014**, *43*, 15028-15037.

[11] a) S. Das, R. R. Rodrigues, R. W. Lamb, F. Qu, E. Reinheimer, C. M. Boudreaux, C. E. Webster, J. H. Delcamp, E. T. Papish, *Inorg. Chem.* **2019**, *58*, 8012-8020; b) J. Agarwal, T. W. Shaw, C. J. Stanton, 3rd, G. F. Majetich, A. B. Bocarsly, H. F. Schaefer, 3rd, *Angew. Chem. Int. Ed.* **2014**, *53*, 5152-5155; c) T. Jin, D. He, W. Li, C. J. Stanton, S. A. Pantovich, G. F. Majetich, H. F. Schaefer, J. Agarwal, D. Wang, G. Li, *Chem. Commun.* **2016**, *52*, 14258-14261; d) C. J. Stanton, 3rd, J. E. Vandezande, G. F. Majetich, H. F. Schaefer, 3rd, J. Agarwal, *Inorg. Chem.* **2016**, *55*, 9509-9512; e) J. A. Therrien, M. O. Wolf, B. O. Patrick, *Inorg. Chem.* **2014**, *53*, 12962-12972.

[12] J. D. Froehlich, C. P. Kubiak, *J. Am. Chem. Soc.* **2015**, *137*, 3565-3573.

[13] M. J. T. Frisch, G. W.; Schlegel, H. B.; Scuseria, G. E.; Robb, M. A.; Cheeseman, J. R.; Scalmani, G.; Barone, V.; Petersson, G. A.; Nakatsuji, H.; Li, X.; Caricato, M.; Marenich, A. V.; Bloino, J.; Janesko, B. G.; Gomperts, R.; Mennucci, B.; Hratchian, H. P.; Ortiz, J. V.; Izmaylov, A. F.; Sonnenberg, J. L.; Williams-Young, D.; Ding, F.; Lipparini, F.; Egidi, F.; Goings, J.; Peng, B.; Petrone, A.; Henderson, T.; Ranasinghe, D.; Zakrzewski, V. G.; Gao, J.; Rega, N.; Zheng, G.; Liang, W.; Hada, M.; Ehara, M.; Toyota, K.; Fukuda, R.; Hasegawa, J.; Ishida, M.; Nakajima, T.; Honda, Y.; Kitao, O.; Nakai, H.; Vreven, T.; Throssell, K.; Montgomery, J. A., Jr.; Peralta, J. E.; Ogliaro, F.; Bearpark, M. J.; Heyd, J. J.; Brothers, E. N.; Kudin, K. N.; Staroverov, V. N.; Keith, T. A.; Kobayashi, R.; Normand, J.; Raghavachari, K.; Rendell, A. P.; Burant, J. C.; Iyengar, S. S.; Tomasi, J.; Cossi, M.; Millam, J. M.; Klene, M.; Adamo, C.; Cammi, R.; Ochterski, J. W.; Martin, R. L.; Morokuma, K.; Farkas, O.; Foresman, J. B.; Fox, D. J., Gaussian, Inc., Wallingford, CT, USA, **2016**.

[14] C. Adamo, V. Barone, *J. Chem. Phys.* **1999**, *110*, 6158-6170.

[15] G. Stefan, *Journal of Computational Chemistry* **2006**, *27*, 1787-1799.

[16] S. Grimme, S. Ehrlich, L. Goerigk, *Journal of Computational Chemistry* **2011**, *32*, 1456-1465.

[17] M. Couty, M. B. Hall, *J. Comput. Chem.* **1996**, *17*, 1359-1370.

[18] P. J. Hay, W. R. Wadt, *J. Chem. Phys.* **1985**, *82*, 299-310.

[19] a) C. E. Check, T. O. Faust, J. M. Bailey, B. J. Wright, T. M. Gilbert, L. S. Sunderlin, *The Journal of Physical Chemistry A* **2001**, *105*, 8111-8116; b) W. R. Wadt, P. J. Hay, *J. Chem. Phys.* **1985**, *82*, 284-298.

[20] a) W. J. Hehre, R. Ditchfield, J. A. Pople, *J. Chem. Phys.* **1972**, *56* 2257-2261; b) P. C. Hariharan, J. A. Pople, *Theoret. Chim. Acta* **1973**, *28*, 213-222; c) G. A. Petersson, M. A. Al‐Laham, *J. Chem. Phys.* **1991**, *94*, 6081-6090.

[21] A. D. McLean, G. S. Chandler, *The Journal of Chemical Physics* **1980**, *72*, 5639-5648.

[22] G. A. Petersson, M. A. Al‐Laham, *J. Chem. Phys.* **1991**, *94*, 6081-6090.

[23] A. V. Marenich, C. J. Cramer, D. G. Truhlar, *The Journal of Physical Chemistry B* **2009**, *113*, 6378-6396.

Entry for the Table of Contents

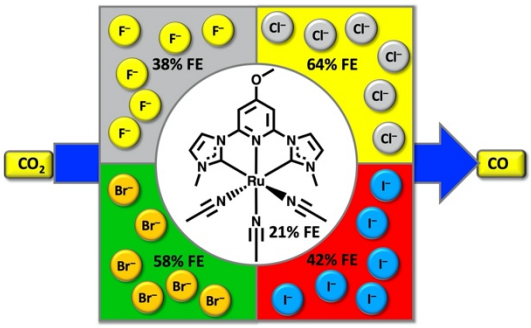

The addition of halide anions to the electrocatalytic CO_2 reduction reaction driven by ruthenium catalysts is found to dramatically influence the Faradaic efficiency and reaction rate. Faradaic efficiencies were found to change from 19% to 91% in the most dramatic case upon addition of Cl^-. Interestingly, computational results reveal an active catalyst with an associated halide is plausible where the halide is trans to the reactive site.

Institute and/or researcher Twitter usernames: @lizpapish, @DelcampGroup, @cedwinwebster